Mine Water Environ (2015) 34:364–374
DOI 10.1007/s10230-014-0285-5

TECHNICAL ARTICLE

# Jarosite Solid Solution Associated with Arsenic-Rich Mine Waters, Macraes Mine, New Zealand

**G. Kerr · J. Druzbicka · K. Lilly · D. Craw**

Received: 4 September 2013 / Accepted: 14 July 2014 / Published online: 5 August 2014


**Abstract** Jarosite is one of the principal precipitates from process waters of the pressure-oxidation autoclave system at the Macraes gold mine, and this jarosite is discharged with the process waters to a tailings impoundment for long-term storage. Dissolved sulfate and arsenate concentrations in the autoclave, inferred from mineralogy, both exceed 0.1 mol/L (≈10,000 mg/L). Coarse-grained (≈1 mm) jarosite crystals, precipitated as mineral scales, provide insight into the mineralogical nature of the jarosite. The jarosite crystals are zoned, with some zones having up to 12 wt% Al, as part of the jarosite-alunite solid solution series. Substitution of up to 1.7 wt% Na for K also occurs. Both the monovalent and trivalent sites in the jarosites have apparent deficiencies (≈10 atm.%) because of protonation of the hydroxyl groups. There is <0.3 wt% As substitution for S in the jarosite anionic site, despite the abundant dissolved As in the autoclave solutions. Instead, jarosite is intergrown with ferric arsenate, and most jarosite growth zones contain numerous small (<20 μm) inclusions of this ferric arsenate. Ferric arsenate precipitation with jarosite occurs as dissolved As decreases by several orders of magnitude during the latter stages of oxidation in the autoclave slurry. The lack of structural As and only minor Na substitution limits the destabilization effects of solid solution within the jarosite in contact with the tailings waters, and jarosite dissolution is expected to be slow. Dissolution is further limited by high (up to 8,000 mg/L) dissolved sulfate in the tailings impoundment. Both jarosite and associated ferric arsenate dissolve incongruently in the surficial environment, yielding ferric oxides/hydroxides, which adsorb As, so that dissolved As is generally <10 mg/L in the tailings water.

G. Kerr · J. Druzbicka · K. Lilly · D. Craw (✉)
Department of Geology, University of Otago,
PO Box 56, Dunedin 9054, New Zealand
e-mail: dave.craw@otago.ac.nz

**Keywords** Ferric arsenate · Scorodite · Alunite · Mine tailings · Autoclave

## Introduction

This study quantifies the arsenic (As) content of the mineral jarosite, a ferric iron sulfate, which precipitates from process waters in a gold ore pressure oxidation system and is discharged to mine tailings. Jarosite and related samples from these mineral scales provided the basis for this study of mineral interactions with process waters and downstream tailings waters. We focus on a single specimen of unusually coarse-grained jarosite (cm scale) that was extracted from mineral scale deposits that crystallised from As-rich solutions in the interior of the pressure oxidation autoclave. Jarosite formed in the natural environment or in experimental studies is generally fine-grained (typically microns to tens of microns; Asta et al. 2010; Giere et al. 2003; Kendall et al. 2013; Savage et al. 2000, 2005). The unusually coarse grain size of the material used for this study facilitated detailed optical and microchemical examination of the internal structure of individual crystals and variations of solid-solution compositions within those crystals. In particular, this coarse-grained material has allowed investigation of whether or not the jarosite is a significant carrier of solid-state As into the mine tailings, where it will remain in long-term contact with the tailings water.

Jarosite (ideal formula $KFe_3[SO4]_2[OH]_6$) is one of the most common secondary minerals in oxidized mine wastes, especially mine wastes that have formed under low pH conditions (Alpers et al. 1994; Bigham 1994; Bigham and Nordstrom 2000; Dutrizac and Jambor 2000; Hudson-Edwards et al. 1999; Lottermoser 2007). Jarosite typically

forms during pyrite oxidation, with associated acidification of mine waters, and is therefore a common precipitate from acid mine drainage (Alpers et al. 1994; Bigham 1994; Bigham and Nordstrom 2000; Hudson-Edwards et al. 1999; Lottermoser 2007). Because jarosite contains ferric iron in its structure, dissolution of jarosite will release that ferric iron, which will generate more acid during subsequent hydrolysis (Alpers et al. 1994; Bigham 1994; Bigham and Nordstrom 2000; Langmuir 1997). Hence, the occurrence and solubility of jarosite in mine waters is a topic of considerable interest when evaluating the environmental stability of mine wastes. Jarosite solubility is affected by substitutions of other elements within its crystal structure, so the specific mineral composition is also of interest when modeling mine waste stability (Casas et al. 2007; Drouet and Navrotsky 2003; Zahrai et al. 2013).

Experimental studies have shown that up to 30 % of the sulfate in jarosite can be replaced by arsenate when precipitated from As-rich solutions, and stabilities of synthetic As-bearing jarosites with up to 10 wt% As have been investigated (Kendall et al. 2013; Paktunc and Dutrizac 2003; Savage et al. 2005). The amount of As that enters the jarosite structure varies widely in nature, from a few hundred ppm to several weight percent (Asta et al. 2010; Giere et al. 2003; Savage et al. 2000). Hence, jarosite dissolution can be a significant source of dissolved As, as well as acidity, in As-rich environments, and jarosite stability in mine wastes is an important issue for this reason as well (Kendall et al. 2013; Paktunc and Dutrizac 2003; Savage et al. 2005).

The jarosite material examined in this study formed during high-temperature (225 °C) oxidation of a slurry of pyrite and arsenopyrite in water. The process water discharges with abundant fine-grained jarosite intimately mixed and intergrown with other fine-grained Fe-As-S bearing material. It has not been possible to determine the As content of the fine-grained jarosite because of this contamination by other material. The environmental stability of jarosite can be affected by solid-solution substitutions within the jarosite structure, and the potential for the jarosite to be a source for dissolved As is an important issue for long-term mine waste storage (Elwood Madden et al. 2012; Kendall et al. 2013; Smith et al. 2006; Zahrai et al. 2013). We show that solid solution As contents of the coarse-grained jarosite are low, and that As principally occurs in intergrown iron arsenate minerals.

## General Setting of the Study Material

The Macraes mine is being developed in a Mesozoic orogenic gold deposit in southern New Zealand (Craw 2002, 2003, 2006). The gold is encapsulated in sulfide minerals, principally pyrite and arsenopyrite, and ore processing involves separation of these sulfides from silicates by flotation. The sulfide content of the ore, c. 1 %, is concentrated tenfold by this flotation process. The resultant sulfide-rich concentrate is then pumped into a pressure-oxidation autoclave at 225 °C, and >3,000 kPa oxygen gas pressure, to oxidize the sulfides and liberate the gold (Craw 2003, 2006; Milham and Craw 2009). The sulfide concentrate passes through the autoclave as a slurry in a continuous feed system, with residence time of about 1 h. Oxidation of the pyrite causes acidification of the slurry to pH <2 (Craw 2006). Iron and arsenic are progressively oxidised through the autoclave, so that Fe(III) and As(V) dominate the process waters at the point of discharge (Fig. 1a). The oxidised concentrate is then passed through a cyanidation system at pH > 10 to extract the gold, and the residue solution is discharged to a tailings impoundment, where it remixes with a slurry of flotation tailings (Craw 2003; Milham and Craw 2009).

The concentrate ore feed to the autoclave is finely ground (<50 μm), and most of the oxidised products are also fine-grained. However, coarser material precipitates as mineral deposits (commonly called "scales") on the autoclave walls and on the agitators that stir the slurry. These mineral scales are made up of numerous mm to cm thick layers with different grain sizes and different combinations of minerals because of locally variable chemistry of the passing slurry. These mineral scales are removed every few months and discarded to the tailings impoundment. Samples of mineral scales collected through the autoclave provide insight into the geochemical processes that occur in the process waters during oxidation, and the minerals that can form during those processes (Craw 2006). Knowledge of this mineralogy is also directly relevant to prediction of potential environmental issues related to mine waters in tailings impoundments (Craw 2003).

## Materials and Methods

More than 100 samples of mineral scales were examined from material collected in the autoclave in 2011–2012. These mineral samples were examined in hand specimen, and mineral content was determined by X-ray diffraction. Many samples contain minerals that, at time of identification, were hydrated. At least some of that hydration may have occurred as the material cooled in the autoclave before sampling, and additional hydration may have occurred during sample transport and preparation for analysis (Craw 2006). Hence, some specific mineral identifications made in the laboratory may not reflect the actual species present while the autoclave was in operation. This is relevant for this study, as ferric arsenate occurs in more

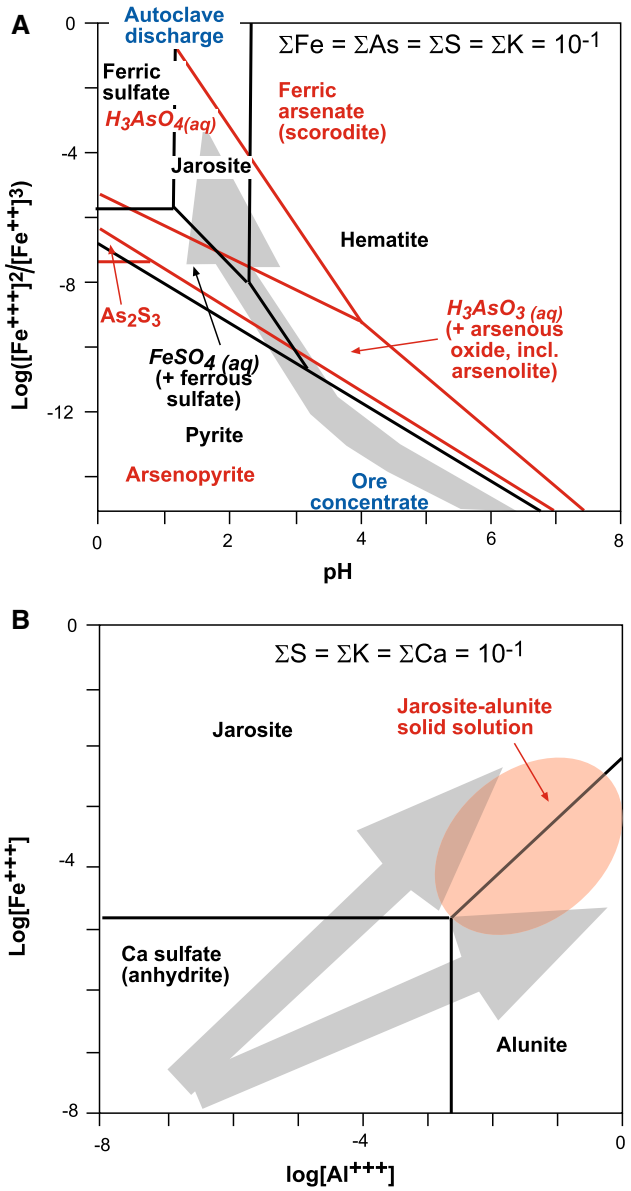


**Fig. 1** Model geochemical and mineralogical phase diagrams (Geochemists Workbench; partly after Craw 2006) for the Macraes mine autoclave oxidation process (*grey arrows*). **a** Progressive oxidation, as measured by ferrous/ferric iron ratio, and pH variations of waters for pyrite (Fe system = *black lines and lettering*) and arsenopyrite (As system = *red lines* and *lettering*) decomposition in the ore concentrate. Aqueous species are in *italics*. Jarosite forms immediately before, and during, discharge from the autoclave. **b** Phase relations among common sulfate minerals in the autoclave, showing the relative stabilities of jarosite and alunite, and the inferred conditions under which solid solution occurs between these minerals (*pink ellipse*)

than one form, including ferric orthoarsenate hydrate ($FeAsO_4 \cdot 3/4H_2O$; Jakeman et al. 1991), scorodite ($FeAsO_4 \cdot 2H_2O$), and amorphous ferric arsenate material, commonly containing sulfur, that is intimately intergrown with amorphous iron oxyhydroxide (Craw 2006; Paktunc et al. 2013). Likewise, calcium sulfate can occur in the processing system as anhydrite, or variably hydrated as bassanite, or gypsum. Hence, we largely use generic names in this paper, particularly for ferric arsenate, unless particular species have been identified. However, there is no evidence that the jarosite, which is the focus of this study, has undergone any hydration or other transformations during cooling and transport. Such transformations would have affected the delicate structures that are preserved in scale specimens, both within and between crystals.

From the available material, one jarosite sample was selected because of its unusually coarse grain size, well-defined layering, and clear spatial separation of mineral phases in some of those layers (Fig. 2a, b). The jarosite examined in this study (Fig. 2a, b) formed in a scale deposit on the autoclave wall three quarters of the way through the autoclave system, about 3 m from the discharge point. The scale sample was extracted from the autoclave in September 2012. The sample yields a clearly-defined jarosite X-ray diffraction pattern, identical to synthetic jarosite (Basciano and Peterson 2007; Fig. 3). The sample also contains subordinate crystalline ferric arsenate, whose X-ray diffraction pattern is largely masked by the dominant jarosite (Fig. 3). At the time of examination, the ferric arsenate had an X-ray diffraction pattern similar to ferric orthoarsenate hydrate.

A portion of the sample was made into a standard polished thin section (30 μm thick), cut perpendicular to the mineral layering (Fig. 2a, b). The scale material is hard and brittle, so only superficial impregnation with epoxy resin was required for thin section production and subsequent polishing. The resultant thin section was examined with a polarized light microscope to select suitable areas for more detailed examination. The polished thin section was coated with carbon and examined with a Zeiss Sigma FEG scanning electron microscope (SEM) with an Oxford Instruments XMax 20 Si drift energy dispersion X-ray detector (EDX). The EDX analytical system was operated at 15 keV for chemical analyses, and lower voltages (down to 5 keV) for some imaging. Element maps were constructed by scanning at 15 keV. Spot analyses were obtained with a tightly focussed beam that interacted with sample volumes with diameters of $\approx 2$ μm. Analytical uncertainties for Na and heavier elements are $\pm 0.2$ wt%. The detection limit for As is $<0.2$ wt% for spot analyses of 1 min.

It is not possible to sample the solutions in the autoclave to measure dissolved concentrations because of the practical and safety issues associated with a hot pressurised system. The solutions change composition rapidly when they discharge, cool, and precipitate dissolved load, and the discharge slurry is rapidly neutralised for further processing, so external measurements are of little value for scientific study of the autoclave processes. Consequently,

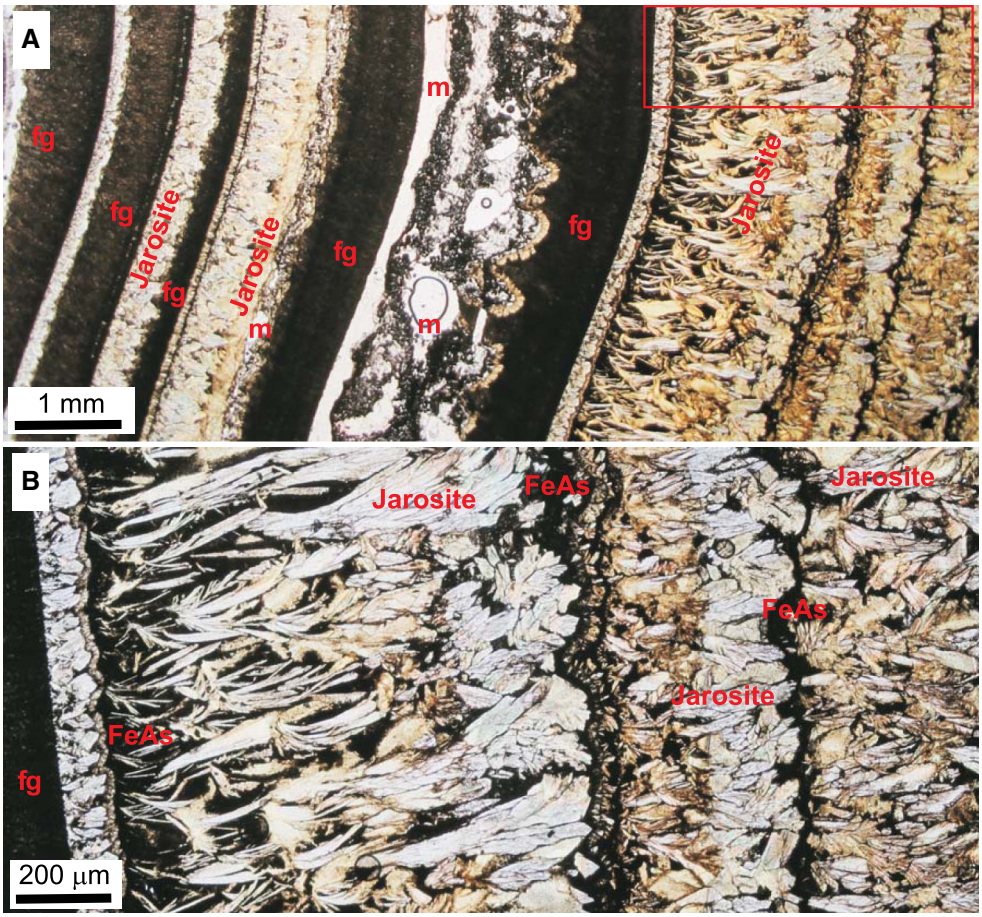


**Fig. 2** Photomicrographs (plane polarized light) of jarosite-rich mineral scale formed in the Macraes mine autoclave. Clear and *pale yellow* material is jarosite, except for zones of mounting medium (m) filling voids in the specimen. Opaque material is ferric arsenate (FeAs), and *dark brown* layers (fg) are fine-grained mixtures of jarosite and ferric arsenate impregnated with dusty hematite. **a** View of multiple layers formed as the scale grew (from *left* to *right*) over several months. **b** Detailed view of scale (*red rectangle* in *top right* of A) showing the layers and intimate intergrowths of jarosite and ferric arsenate

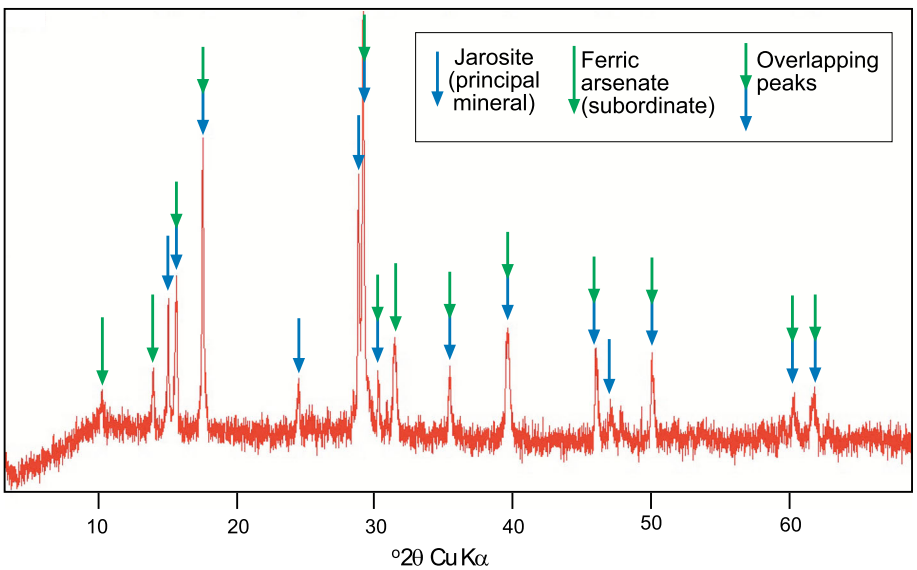


**Fig. 3** X-ray diffraction pattern (Cu Kα radiation) for autoclave scale material shown in Fig. 2, with indicated standard K-jarosite peaks (Basciano and Peterson 2007), and minor ferric orthoarsenate hydrate, whose peaks are largely obscured by the jarosite

solution parameters can merely be estimated from the known stabilities and solubilities of the minerals present. This has been done for the autoclave system using the modelling software package Geochemists Workbench 8.0 (Fig. 1a, b; Craw 2006). Models were run at 200 °C, as this is the highest practical temperature for the database for the minerals relevant to this study.

## Results

### Autoclave Mineralogy

Scale mineralogy shows that the first half of the autoclave is dominated by Ca sulfate, alunite ($KAl_3[SO4]_2[OH]_6$), and ferrous sulfates, and the principal As minerals are As(III) oxides (arsenolite or claudetite, $As_2^{III}O_3$). The iron and As minerals are all the result of incomplete oxidation of the pyrite and arsenopyrite (Fig. 1a). More advanced oxidation occurs in the downstream half of the autoclave, where ferric sulfates can precipitate (Fig. 1a; Craw 2006). Some scale in the downstream half of the autoclave contain abundant jarosite, some contain alunite, and some contain both minerals (Fig. 1b; Craw 2006). The slurry discharging from the autoclave contains crystalline jarosite, Ca sulfate, and ferric arsenate, and abundant amorphous Fe-As-S bearing material (Craw 2006). The jarosite in the oxidised concentrate that discharges from the autoclave is fine-grained (typically 1–10 μm) and intimately intergrown with the ferric arsenate and Ca sulfate precipitates. Despite the strong oxidative environment of the autoclave, and precipitation of $Fe^{III}$ and $As^{V}$ minerals, some dissolved $Fe^{II}$, and possibly $As^{III}$, persist in the discharge waters (Craw 2003). There are apparently steep and complex redox gradients and/or variable chemical disequilibrium because of reaction kinetics within the autoclave system.

The studied scale material was confirmed to be jarosite by light microscopy, X-ray diffraction, electron backscatter imaging, and microchemical analysis (Figs. 2, 3, 4, 5 and 6). The jarosite scale sample is laminated on the 1 mm scale, with interlayered brown and pale green horizons visible in hand specimen. The brown colour of some layers is a result of disseminated dusty hematite, and rare bright red layers reflect a higher proportion of hematite. Jarosite is pale green to white, with the greenish tinges resulting from scattered ferric arsenate. Thin (≈0.5 mm) darker green laminae are richer in ferric arsenate than the paler jarosite-dominated laminae. Coarse-grained jarosite layers are made up of elongate crystals (0.1–0.5 mm) that have grown perpendicular to the underlying layers (Fig. 2a, b). Crystals are complexly intergrown, and impinge on each other, but some terminated crystals occur within these masses (Fig. 4a).

### Jarosite Compositional Zoning

Distinct compositional growth zoning is visible in some jarosite crystals in thin section and in electron images (Figs. 4a, 5a). This prominent zoning reflects variations in Fe and Al contents; the complementary nature of these variations (Fig. 5b, c), with low Fe zones corresponding to high Al, has been quantified with spot analyses across the crystal in Fig. 5a, and plotted in Fig. 6a. These data show that most jarosite contains 1–2 wt% Al, but that some zones have up to 12 wt% Al (Fig. 6a). Individual growth zones have essentially constant compositions, and this, combined with the complementarity of the Fe and Al variations between zones, implies that the Al is in solid solution in the trivalent site in jarosite, as part of the jarosite-alunite series. While jarosite and alunite have been identified as separate minerals in the scales by X-ray diffraction, reflecting locally different solution compositions in the autoclave (Craw 2006), the mineralogical and geochemical boundary between these phases is diffuse because of the solid solution identified herein (Fig. 1b).

Potassium and Na content of the jarosite also vary in a complementary manner, and presumably reflect solid solution in the monovalent ion site of the jarosite between growth zones, with Na ranging up to 1.7 wt% (Figs. 5e, 6b). The Na variations are too subtle to be detectable via element mapping (Fig. 5f). The prominent Al-rich zones near the outside of the crystal in Fig. 5a have the highest K content, but the other variations in K content are not correlated with variations in Fe and Al content (Fig. 6a, b).

Calculated formulae for the jarosite analyses, assuming 2.00 sulfate ions, result in an apparent deficiency in the monovalent and trivalent sites of most of the analyses, compared to ideal jarosite (Fig. 7). This type of deficiency has been noted for many natural jarosites, and has been attributed to protonation of the hydroxyl groups (Basciano and Peterson 2007; Bigham 1994; Bigham and Nordstrom 2000; Ripmeester et al. 1986). The deficiency in the sites ranges up to ≈0.3 atomic units (Fig. 7). The calculated ideal jarosite components of the analysed crystal zones show wide variations, reflecting the two largely independent solid solution substitutions described above (Fig. 7).

### Arsenic Distribution

A notable feature of the jarosite crystals examined in detail is that they contain little or no detectable As in solid solution (Fig. 5d). Some spot analyses indicated up to 0.3 wt% As, but most spots were below 0.2 wt%. There has been no As-related shift in the d-spacings of jarosite structure, as quantified in the jarosite X-ray diffraction patterns (cf. Kendall et al. 2013; Paktunc and Dutrizac 2003; Savage et al. 2005). Arsenic is present only as ferric

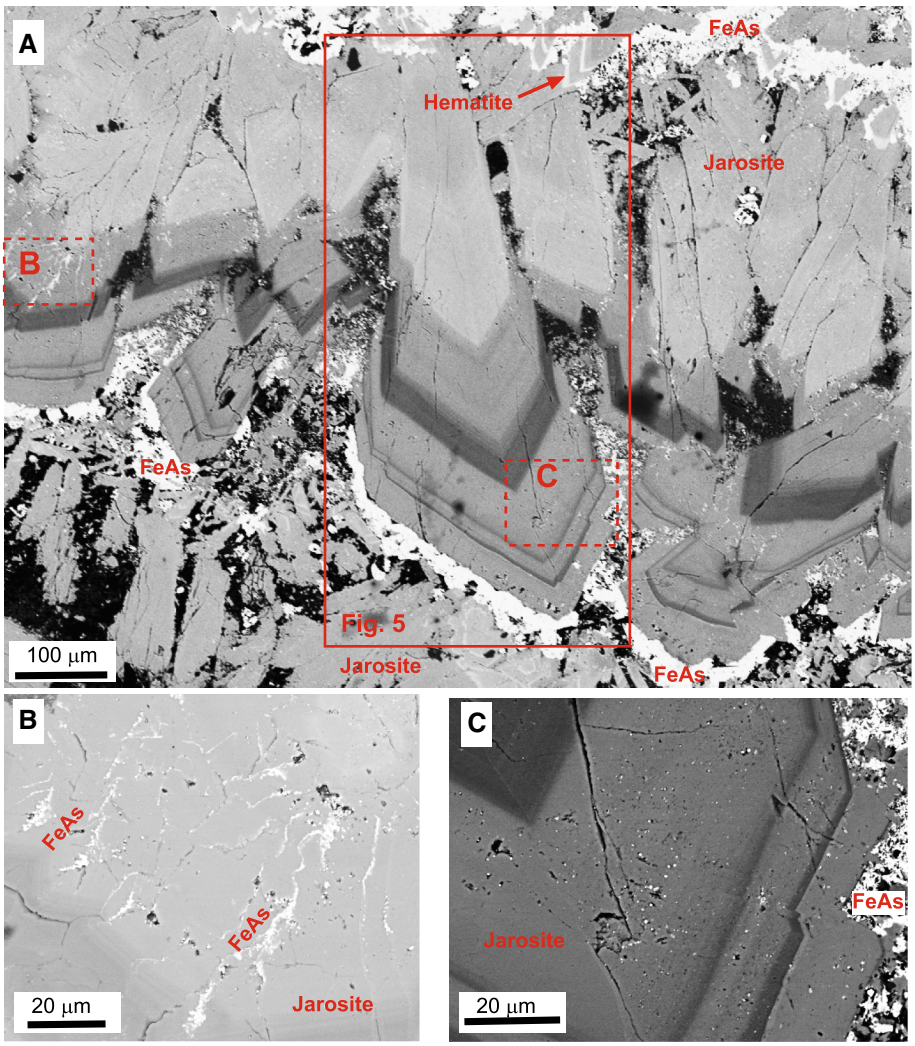


**Fig. 4** Backscatter electron images of jarosite crystals in Macraes mine autoclave scale. Jarosite is shades of *grey* (*darker* higher Al content), *white* ferric arsenate or hematite, and *black* mounting medium. **a** View of a set of impinging crystals that have grown progressively from *top to bottom*, with intervening layers of ferric arsenate, and minor fine layers of hematite (*top centre*). **b** Closer view of area indicated in A (*dashed red box*) with fine veinlets of ferric arsenate at a high angle to growth zones in jarosite. **c** Closer view of area indicated in **a** (*dashed red box*), with micron scale ferric arsenate and hematite inclusions scattered through the jarosite

arsenate within and around the jarosite crystals (Figs. 2a, b, 4a–c). Ferric arsenate forms discrete layers between jarosite laminae, and also fills interstices between jarosite crystals in jarosite-rich laminae (Figs. 2a, b, 4a). In addition, numerous anhedral inclusions of ferric arsenate are scattered through jarosite crystals, and these are more abundant in some zones of the jarosite crystals than in others (Fig. 4a, c). Irregular cracks in jarosite crystals are locally filled with ferric arsenate as well (Fig. 4b).

## Discussion

### Arsenic in Jarosite

The dissolved As content of solutions in the autoclave can reach very high levels (>0.1 mol/L), so that As(III) oxide minerals such as arsenolite can precipitate (Figs. 1a, 8). In this As-rich environment, significant solid solution of As in jarosite is expected (Paktunc and Dutrizac 2003; Savage et al. 2005, 2009). Experimental synthesis suggests that jarosite can preferentially partition As into its structure at higher As/S ratios than the starting solution (Savage et al. 2005). Arsenic can enter the jarosite crystal structure by replacing sulfate ions ($SO_4^{2-}$) with arsenate ions ($AsO_4^{3-}$), with compensating addition of hydrogen ions (Paktunc and Dutrizac 2003; Savage et al. 2005). Hence, As solid solution in jarosite occurs under oxidized conditions where $As^V$ prevails (Kendall et al. 2013; Paktunc and Dutrizac 2003; Savage et al. 2005).

Geochemical modelling suggests that high As concentrations occur in the Macraes mine autoclave (>0.1 mol/L; ≈10,000 mg/L), with the highest dissolved As concentrations occurring when the As from arsenopyrite has been only partially oxidized, to yield $As^{III}$ ($H_3AsO_3$; Fig. 8). Under more oxidized conditions, with abundant $As^V$ ($H_3AsO_4$; Fig. 8), the modelling suggests that ferric arsenate precipitates from solution and the dissolved As concentrations drops by one or more orders of magnitude (Fig. 8). The drop in dissolved As concentrations implied

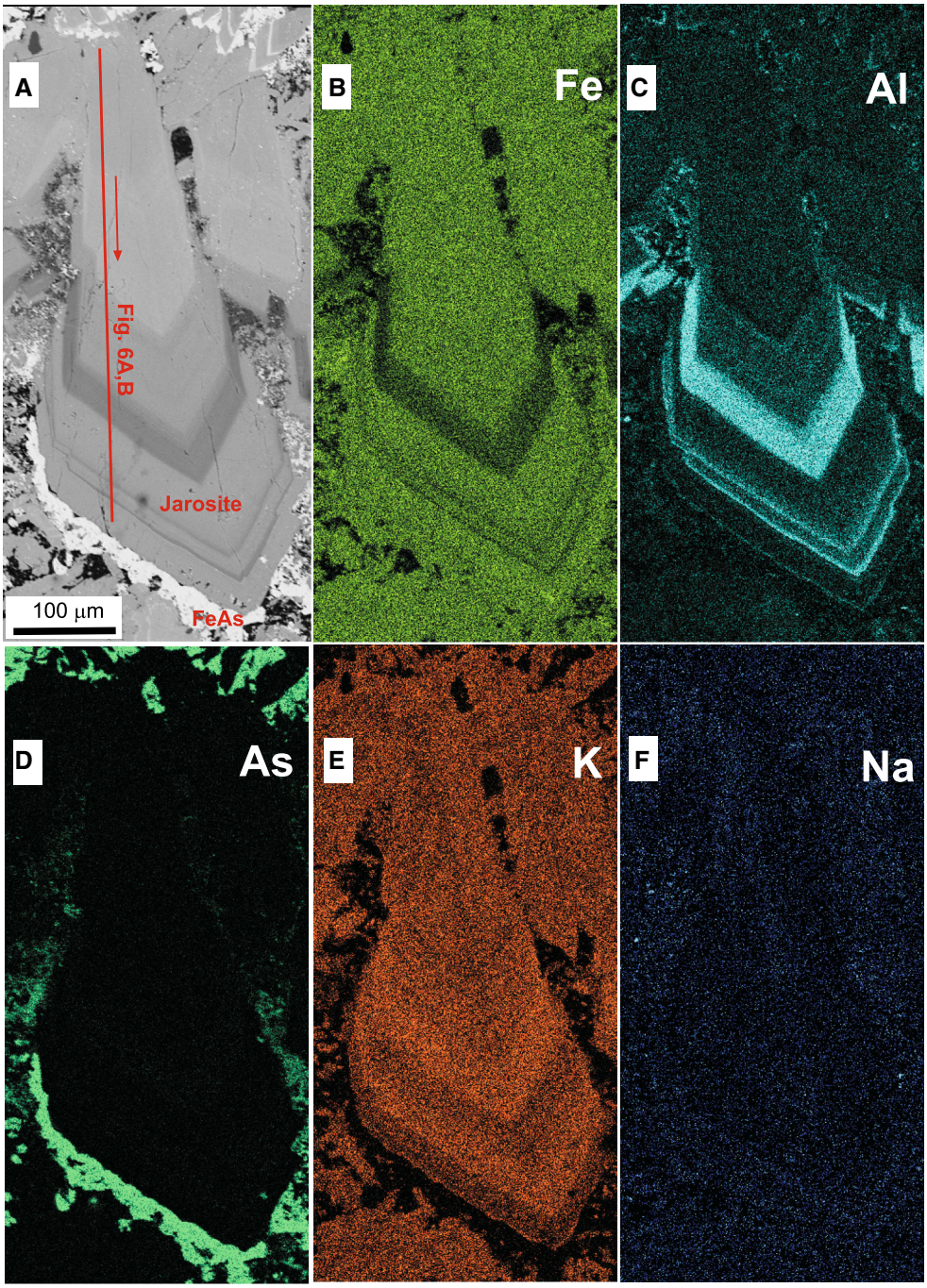


**Fig. 5** Element maps of jarosite crystals and associated ferric arsenate. **a** Backscatter electron image to show the location of the maps (area indicated in Fig. 4a, *red rectangle*). The locations of analytical profiles in Fig. 6 are indicated. **b** Iron map. **c** Aluminium map. **d** Arsenic map. **e** Potassium map. **f** Sodium map

by the model in Fig. 8 must occur rapidly (minutes to tens of minutes) over a short distance (metres or less) within the autoclave, as suggested by downstream changes from arsenolite-bearing to ferric arsenate-bearing scale deposits. Solid solution substitution of $As^V$ into the jarosite structure is apparently limited to the oxidised part of the autoclave.

The sudden decrease of dissolved $As^V$ concentrations in the oxidizing ore concentrate slurry, implied by scale mineralogy and geochemical model (Fig. 8) leads to precipitation of abundant, fine-grained ferric arsenate, which is a significant component of the material discharged. Some of this fine-grained ferric arsenate has apparently been incorporated as inclusions in the growing jarosite crystals, along with hematite (Fig. 4a–c). There is additional fine-grained ferric arsenate that fills cracks that cut across the jarosite growth structures (Fig. 4b). This later-stage mineralization process has added additional fine-grained ferric arsenate particulate material to the jarosite crystals. Hence, the jarosite in this study contains As that has been physically incorporated as a separate ferric arsenate phase, rather than as the solid solution As that is commonly observed elsewhere.

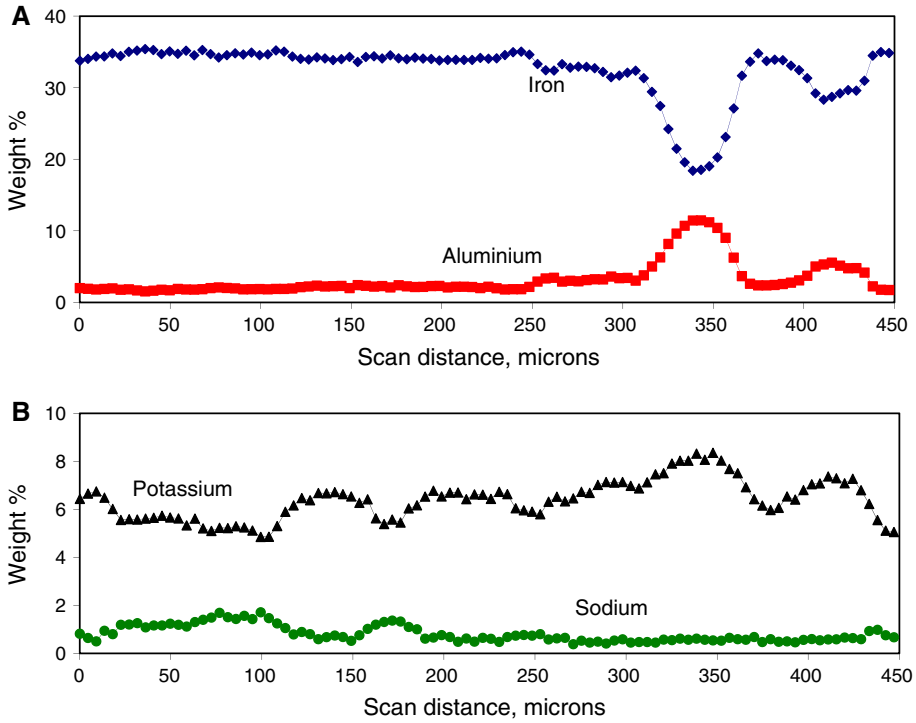


**Fig. 6** Concentrations of major elements in a traverse across a jarosite crystal (line shown in Fig. 5A, with direction of traverse). **a** Variations in Fe and Al contents. **b** Variations in K and Na contents

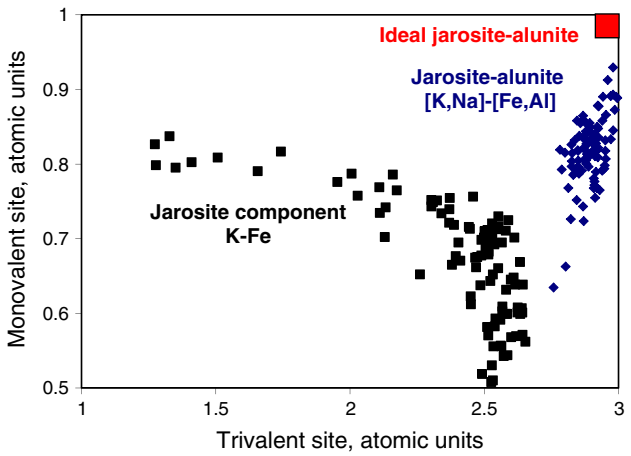


**Fig. 7** Plots of the analytical data depicted in Fig. 6, after recalculation to a mineral formula assuming the sulfur content = 2.00 atomic units, presented in comparison to ideal jarosite (*red box*). *Blue diamonds* are the total results for trivalent Fe + Al site versus monovalent K + Na site. *Black squares* show the K-jarosite component of the analyses

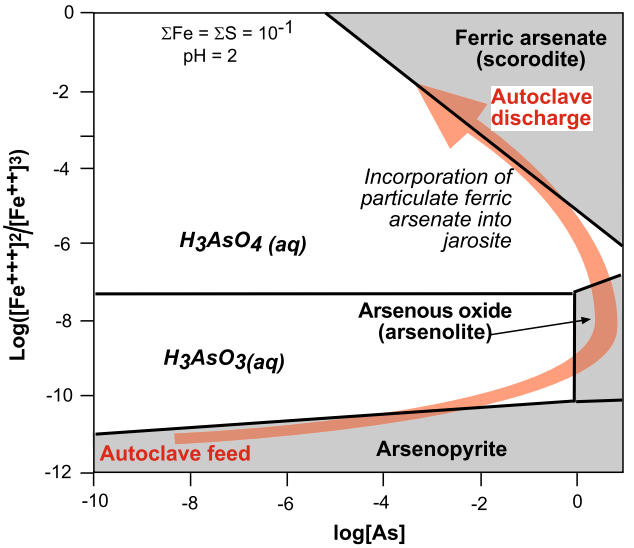


**Fig. 8** Model variations in dissolved As concentrations during progressive oxidation (*red arrow*) of arsenopyrite to ferric arsenate in the Macraes mine autoclave. Solid fields are *grey*. Model was constructed with Geochemists Workbench by suppressing phases irrelevant to arsenic in the autoclave system

## Environmental Stability of Jarosite

The tailings impoundment at Macraes mine is the ultimate destination for the autoclaved material (apart from the gold), including the jarosite-rich slurry and scales. The tailings impoundment contains water with a pH near 6, despite the abundant carbonate minerals in accompanying flotation tailings, because of on-going oxidation and hydrolysis of minor remnants of dissolved ferrous iron (Craw 2003). Dissolved sulfate concentrations in tailings impoundment waters are typically 3,000–6,000 mg/L or 0.03–0.06 mol/L (Fig. 9). Since there has been around a ten-fold dilution in the tailings impoundment by flotation tailings slurry, the discharge waters from the autoclave

probably had dissolved sulfate concentrations >0.1 mol/L, similar to that inferred from minerals in the autoclave (Fig. 1a). As the tailings waters percolate through the impoundment structure, the dissolved sulfate concentration drops because of gypsum precipitation (Craw 2003), and waters seeping from the impoundment have ≈2,000 mg/L dissolved sulfate (Fig. 9).

Jarosite dissolves relatively slowly at pH 6 compared to alkaline or low pH (<2) conditions and the dissolution is incongruent, yielding solid ferric oxide/hydroxide phases (Elwood Madden et al. 2012; Smith et al. 2006). The dissolution reaction (Elwood Madden et al. 2012) is of the form:

$$KFe_3[SO_4]_2[OH]_6 + 3OH^- = 3Fe[OH]_3 + K^+ + 2SO_4^{2-} \quad (1)$$

This dissolution reaction is further limited by the high dissolved sulfate in the mine tailings waters (Fig. 9). The presence of Na substituting for K in the monovalent site of jarosite facilitates faster dissolution, and 100 % substitution by Na causes a threefold increase in dissolution rates (Zahrai et al. 2013). The small amount of Na substitution in jarosites in this study (≈20 at. %; Fig. 7) has only a minor effect on overall stability of the jarosite. Calculated dissolution lifetimes of 1 mm jarosite particles at pH 6 are ≈100 years for low sulfate environmental solutions (Zahrai et al. 2013). High dissolved sulfate and potential particle armouring by ferric oxide precipitates (Eq. 1; Elwood Madden et al. 2012; Kendall et al. 2013) should substantially increase this particle lifetime. Hence, jarosite dissolution in the Macraes mine tailings impoundment will be very slow and will probably occur on a time scale of hundreds of years.

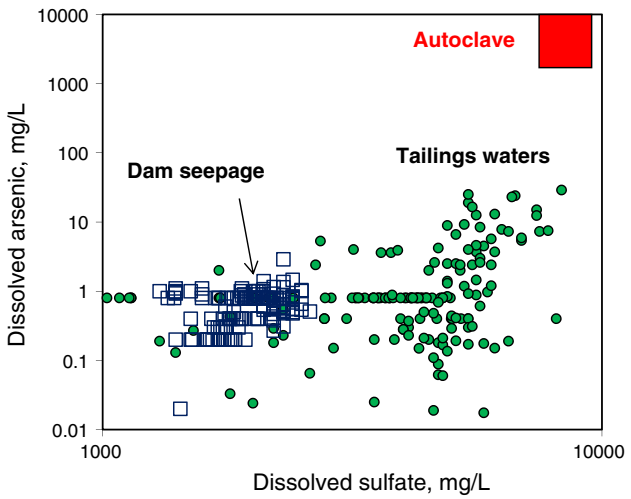


**Fig. 9** Comparison of dissolved arsenic and dissolved sulfate contents (log scales) of mine waters in the Macraes mine system. Dissolved arsenic and dissolved sulfate were approximately equal at ~10,000 mg/L in the middle of the autoclave (*red box*). Arsenic has since been progressively precipitated and/or adsorbed to a much greater extent than sulfate, so that the tailings impoundment waters (*green circles*) have lower dissolved As, and waters seeping from the tailings dam (*blue squares*) have even lower dissolved As, as well as lower sulfate

The presence of solid solution arsenic in jarosite causes faster dissolution, combined with release of the As (Kendall et al. 2013). Hence, the absence of solid solution As in the jarosite in the Macraes mine tailings is a positive feature from an environmental perspective. Nevertheless, the associated ferric arsenate (Figs. 2a, b; 4a–d) is also significantly soluble in mine waters (Krause and Ettel 1989; Langmuir et al. 2006; Paktunc and Bruggeman 2010; Paktunc et al. 2008, 2013). Further, dissolution of the jarosite will progressively expose more of the intimately intergrown ferric arsenate (e.g., Fig. 4b–d) to environmental waters. However, ferric arsenate dissolution at pH 6 is incongruent and yields ferric oxide/hydroxide precipitates and residues, in a similar manner to jarosite dissolution (Eq. 1). These ferric oxide/hydroxide precipitates and residues adsorb As released from the dissolution reactions (Asta et al. 2010; Giere et al. 2003; Kendall et al. 2013; Roddick-Lanzilotta et al. 2002). Adsorption of As to ferric hydroxide is an important mechanism for limiting dissolved As, and this adsorption has contributed to lowering of dissolved As concentrations in the Macraes mine tailings impoundment to <30 mg/L (Fig. 9; Craw 2003; Milham and Craw 2009). Adsorption of As to ferric hydroxides in waters seeping beneath the tailings impoundment generally restricts dissolved As to <5 mg/L (Fig. 9; Roddick-Lanzilotta et al. 2002).

## Conclusions

Coarse-grained jarosite precipitates from process waters in the pressure-oxidation autoclave (225 °C) at the Macraes mine, and this coarse-grained material provides insights into the mineralogical nature of jarosite, which is a principal mineral product in the processing system discharge waters. The coarse-grained jarosite includes growth zones of differing composition, primarily as a result of solid solution substitution of Al (up to 12 wt% Al, or 10 at.%) for Fe in the trivalent site in the jarosite-alunite mineral series. In addition, there has been up to 20 at.% substitution of Na for K in the monovalent site. Jarosite dissolves slowly in the surface environment at pH 6 in high sulfate waters, the conditions prevailing in the Macraes tailings impoundment that stores the jarosite-bearing mine wastes. The effects on dissolution rates of the substitution of minor Na for K in the structure are negligible, and jarosite particles can be expected to survive for hundreds of years.

Dissolved $As^{III}$ concentrations in the autoclave solutions can be >0.1 mol/L during the oxidation process, similar to dissolved sulfate concentrations. Further oxidation to $As^{V}$ causes precipitation of ferric arsenate and associated decrease of dissolved As, possibly by several orders of magnitude locally. The resultant relatively low dissolved $As^{V}$ in the process waters ensures that arsenate ions do not replace sulfate ions in the jarosite structure, and solid solution As in the studied jarosite is not detectable (<0.3 wt%). Both jarosite and ferric arsenate dissolve incongruently in mine waters in the tailings impoundment, yielding ferric oxide/hydroxide, which adsorbs As from solution. The combination of high temperature, high redox, ferric arsenate precipitation in the autoclave, and adsorption of As from solution in the tailings impoundment under surficial conditions, ensures that dissolved As in the mine water environment generally remains below 10 mg/L. Hence, arsenic is selectively retained with the solids, while dissolved sulfate concentrations remain high in the mine waters (1,000–8,000 mg/L).

**Acknowledgments** This research was financed by the University of Otago and NZ Ministry of Business, Innovation and Employment. This project would have been impossible without the ongoing enthusiasm and logistical support for research on the Macraes mine site by Oceana Gold Ltd, which is much appreciated. In particular, discussions with Geua Mola and Quenton Johnston were very helpful. Constructive comments by two anonymous referees substantially improved the presentation of the paper.

## References

Alpers CN, Blowes DW, Nordstrom DK, Jambor JL (1994) Secondary minerals and acid mine water chemistry. In: Jambor JL, Blowes DW (eds) The environmental geochemistry of sulfide mine wastes. Mineral Association Canada Short Course Handbook 22:247–270

Asta MP, Ayora C, Roman-Ross G, Cama J, Acero P, Gault AG, Chamock JM, Bardelli F (2010) Natural attenuation of arsenic in the Tinto Santa Rosa acid stream (Iberian Pyritic Belt, SW Spain): the role of iron precipitates. Chem Geol 271:1–12

Basciano LC, Peterson RC (2007) Jarosite-hydronium jarosite solid-solution series with full iron site occupancy: mineralogy and crystal chemistry. Am Mineral 92:1464–1473

Bigham JM (1994) Mineralogy of ochre deposits formed by sulphide oxidation. In: Jambor JL, Blowes DW (Eds), The Environmental Geochemistry of Sulfide Mine-Wastes, Mineral Association Canada Short Course 22:103–132

Bigham JM, Nordstrom DK (2000) Iron and aluminium hydroxysulfates from acid sulphate waters. In: Alpers CN, Jambor JL, Nordstrom DK (Eds) Sulfate Minerals: Crystallography, Geochemistry, and Environmental Significance. Rev Mineral Geochem 40:351–403

Casas JM, Paipa C, Godoy I, Vargas T (2007) Solubility of sodium-jarosite and solution speciation in the system Fe(III)–Na–$H_2SO_4$–$H_2O$ at 70 °C. J Geochem Explor 92:111–119

Craw D (2002) Geochemistry of late metamorphic hydrothermal alteration and graphitisation of host rock, Macraes gold mine, Otago Schist, New Zealand. Chem Geol 191:257–275

Craw D (2003) Geochemical changes in mine tailings during a transition to pressure–oxidation process discharge, Macraes Mine, New Zealand. J Geochem Explor 80:81–94

Craw D (2006) Pressure-oxidation autoclave as an analogue for acid-sulphate alteration in epithermal systems. Miner Depos 41:357–368

Drouet C, Navrotsky A (2003) Synthesis, characterization, and thermochemistry of K-Na–H3O jarosites. Geochim Cosmochim Acta 67:2063–2076

Dutrizac JE, Jambor JL (2000) Jarosites and their applications in hydrometallurgy. In: Alpers CN, Jambor JL, Nordstrom DK (Eds), Sulfate Minerals: Crystallography, Geochemistry, and Environmental Significance. Rev Mineral Geochem 40:405–452

Elwood Madden ME, Madden AS, Rimstidt JD, Zahrai SK, Kendall MR, Miller MA (2012) Jarosite dissolution rates and nanoscale mineralogy. Geochim Cosmochim Acta 91:306–321

Giere R, Sidenko NV, Lazareva EV (2003) The role of secondary minerals in controlling the migration of arsenic and metals from high-sulfide wastes (Berikul gold mine, Siberia). Appl Geochem 18:1347–1359

Hudson-Edwards KA, Schell C, Macklin MG (1999) Mineralogy and geochemistry of alluvium contaminated by metal mining in the Rio Tinto area, southwest Spain. Appl Geochem 14:55–70

Jakeman RJB, Kweicen MJ, Reiff WM, Cheetham AK, Toradi CC (1991) A new ferric orthoarsenate hydrate–structure and magnetic-ordering of $FeAsO_4 \cdot 3/4H_2O$. Inorg Chem 30: 2806–2811

Kendall MR, Madden AS, Elwood Madden ME, Hu Q (2013) Effects of arsenic incorporation on jarosite dissolution rates and reaction products. Geochim Cosmochim Acta 112:192–207

Krause E, Ettel VA (1989) Solubilities and stabilities of ferric arsenate compounds. Hydrometall 22:311–337

Langmuir D (1997) Aqueous environmental geochemistry. Prentice-Hall, Upper Saddle River

Langmuir D, Mahoney J, Rowson J (2006) Solubility products of amorphous ferric arsenate and crystalline scorodite ($FeAsO_4 \cdot 2H_2O$) and their application to arsenic behaviour in buried mine tailings. Geochim Cosmochim Acta 70:2942–2956

Lottermoser BG (2007) Mine Wastes: Characterization, Treatment and Environmental Impacts. 2nd edn. Springer, Berlin, Germany

Milham L, Craw D (2009) Antimony mobilization through two contrasting gold ore processing systems, New Zealand. Mine Water Environ 28:136–145

Paktunc D, Bruggeman K (2010) Solubility of nanocrystalline scorodite and amorphous ferric arsenate: implications for stabilization of arsenic in mine wastes. Appl Geochem 25:674–683

Paktunc D, Dutrizac JE (2003) Characterization of arsenate-for-sulfate substitution in synthetic jarosite using X-ray diffraction and X-ray absorption spectroscopy. Can Mineral 41:905–919

Paktunc D, Dutrizac J, Gertsman V (2008) Synthesis and phase transformations involving scorodite, ferric arsenate and arsenical ferrihydrite: implications for arsenic mobility. Geochim Cosmochim Acta 72:2649–2672

Paktunc D, Majzlan J, Palatinus L, Dutrizac J, Klementova M, Poirier G (2013) Characterization of ferric arsenate-sulfate compounds: implications for arsenic control in refractory gold processing residues. Am Mineral 98:554–565

Ripmeester JA, Ratcliffe CI, Dutrizac JE, Jambor JL (1986) Hydronium in the alunite-jarosite group. Can Miner 24:435–447

Roddick-Lanzilotta AJ, McQuillan AJ, Craw D (2002) Infrared spectroscopic characterisation of arsenate(V) ion adsorption from mine waters, Macraes Mine, New Zealand. Appl Geochem 17:445–454

Savage K, Tingle T, O'Day P, Waychunas G, Bird D (2000) Arsenic speciation in pyrite and secondary weathering phases, Mother Lode Gold District, Tuolumne County, California. Appl Geochem 15:1219–1244

Savage K, Bird D, O'Day P (2005) Arsenic speciation in synthetic jarosite. Chem Geol 215:473–498

Smith A, Hudson-Edwards K, Dubbin W, Wright K (2006) Dissolution of jarosite [$KFe_3(SO_4)_2(OH)_6$] at pH 2 and 8: insights from batch experiments and computational modeling. Geochim Cosmochim Acta 70:608–621

Zahrai SK, Elwood Madden ME, Madden AS, Rimstidt JD (2013) Na-jarosite dissolution rates: the effect of mineral composition on jarosite lifetimes. Icarus 223:438–443